

Estimation of contents of iron oxides using geostatistics in two hillslope curvatures of an Alfisol under sugarcane cultivation

João Fernandes da Silva Júnior^{1*}, José Marques Júnior¹, Livia Arantes Camargo¹, Daniel De Bortoli Teixeira¹, Alan Rodrigo Panosso², Gener Tadeu Pereira¹

¹State University of São Paulo (UNESP), Jaboticabal, São Paulo, Brazil, P.O.Box: 4111, Jaboticabal 31587-77871, Brazil

²State University of São Paulo (UNESP), Ilha Solteira, São Paulo, Brazil, 56, Centro15385-000, Ilha Solteira, SP, Brazil

*Corresponding author: joajrsilva@yahoo.com.br

Abstract

The spatial characterization of Fe oxides (hematite and goethite content) has usually been made by ordinary kriging (OK) considering the variogram parameters. However, OK softens local details of the spatial variation, overestimating small values and underestimating high ones. Thus, Trans-Gaussian Kriging (TGK) becomes an alternative to have a robust estimation of the variogram, reducing outlier effects. The objective of this study was to evaluate OK and TGK algorithm performances in estimating and mapping goethite and hematite iron oxides in two hillslope curvatures on an Alfisol in Catanduva, São Paulo State, Brazil. Two sampling areas were selected, one concave landscape and another convex landscape. Then, over each area, a 1st sample grid with regular spacing of 10 × 10 m, totaling 121 sample points of soil per area, was selected. The mineralogical analysis was performed in each sample to determine hematite and goethite contents. Moreover, to meet TGK criteria, data were previously converted to standard normal transformation, whereas OK data were not transformed. The TGK estimates presented improved accuracy mapping from 0.84 to 11.1% for the Gt and from 8.23 to 0.76% for the Hm content in concave and convex hillslope curvature, respectively. In general, the TGK estimates reproduced the best results. Moreover, the conditional cumulative distribution function and experimental variogram were better reproduced by TGK estimates than OK. The TGK is recommended for estimation of a more stable robust variogram in Fe oxide mapping with strong variability, when higher efficiency and accuracy are required. Hillslope curvatures influenced the interpolation efficiency and accuracy of interpolation. Relief classification is as much important as the variogram modeling for a greater efficiency and it would improve digital modeling of Fe oxides. The OK maps for Fe oxides should be cautiously used due to its uncertainty, especially in different hillslope curvatures mappings.

Keywords: Mapping; Pedometric; Robust kriging; Goethite; Hematite.

Abbreviations: CV_Coefficient of Variation; DEM_Digital Elevation Model; DSM_Digital soil mapping; GPS_Global Positioning System; MSE_Mean Square Error; R²_Correlation Coefficient; RSS_Residual Sum of Square; OK_Ordinary Kriging; TGK_Trans-Gaussian Kriging.

Introduction

Goethite (Gt) and hematite (Hm) iron oxides are good pedogenetic indicators for tropical soils (Schwertmann and Taylor, 1989; Kämpf and Curi, 2000; Bigham et al., 2002). Their spatial variability is correlated with soil physical and chemical spatial variability and influenced by relief (Camargo et al., 2012, 2013a,b). Therefore, the spatial variability characterization of these oxides becomes an important tool to identify and to map homogeneous soil areas at varied scales, allowing the setting of soil sampling strategies (Goovaerts, 2001, Campos et al., 2006, Camargo et al., 2012, 2013a,b). In this regard, the recommended tool for spatial variability characterization and Fe oxides mapping within landscape is geostatistics (Wilding and Drees 1983), not only to produce spatial distribution maps, but also to assess efficiency and accuracy, in which they are being generated by the geostatistical methods. From the most commonly used methods to determine various spatially related quantities; Ordinary Kriging (OK) is widely used for soil attributes. The OK may characterize one or more variability parameters in space and/or time, thus being useful

for precision agriculture management. The prediction by OK does not require a normal distribution of data. However, input data normality is crucial for map interpolation with a strong sense of security (Kerry and Oliver, 2007). Several authors are already considering a normal standardized transformation with the use of kriging methods (Goovaerts, 1999). The corresponding spatial interpolation of kriging is called Trans-Gaussian Kriging (TGK) (Cressie 1993). In the literature, there are many examples of the TGK, which provides a robust estimation of the variogram, reducing outlier effects (Emery, 2006; Robinson and Metternicht, 2006; Yamamoto and Chao, 2009; Silva Júnior et al., 2012a,b). It is believed that TGK may supply more accurate estimations and maps of Fe oxides, helping to identify cause-effect relationships of them with crop yield and quality. The aim of this study was to evaluate OK and TGK algorithm performance in estimating and mapping of the goethite and hematite Fe oxides on two hillslope curvatures on an Alfisol in Catanduva, São Paulo State, Brazil.

Results and Discussion

Soil properties

The Fe oxide contents presented the highest mean values in the convex hillslope curvature (Table 1). This result can be explained by the landscape position that favors intense leaching, weathering and erosion. Within this area, A+E horizon thickness was smaller, which made each sampled layer to be more influenced by Bt horizon, with greater content of clay and Fe oxides (Camargo et al., 2013a). Montanari et al. (2010) found similar results, where they characterized the clay fraction mineralogy of an Oxisol at different relief features, and found the highest oxide concentrations in convex hillslope. The lowest mean values of Fe oxide contents in concave hillslope curvature may be because it favors a lower soil-weathering rate. The data supported the normality hypothesis for the goethite (Gt) in both hillslope curvatures ($p > 0.01$; Anderson-Darling test); and for hematite (Hm) in convex curvature ($p > 0.05$; Anderson-Darling test). According to the classification proposed by Warrick and Nielsen (1980), oxide content coefficients of variation (CV) indicated a medium variability for both hillslope curvatures. The CVs for the Gt and Hm contents were higher in the concave than convex area. Cunha et al. (2005) and Montanari et al. (2010) explained that this high variability is due to the position, where the material from higher ground is deposited. Additionally, there is a greater variability of Gt in relation to Hm contents for both hillslope curvatures. These results agree with those found by Camargo et al. (2008) in Oxisols. As reported by Inda Júnior and Kämpf (2005), a lower variation of Hm is due to greater specificity in this mineral formation than in Gt, which is more sensitive to environmental changes.

Spatial variability characterization of Fe oxides

Mathematical models adjusted to the variograms by geostatistics techniques showed a spatial dependence structure, and the spherical model provided the best fit in both areas (Table 2). This model also best fitted all standardized variogram. Moreover, such model is widely used in spatial variability studies in soil science (McBratney and Webster, 1986). Value range found for the Gt and Hm variograms were higher in the convex hillslope curvature, with and without transformation. This finding indicates large spatial continuity within the area compared to concave curvature. This spatial continuity can be attributed to the shallow and lateral flow of drainage water in convex areas, generating specific environments that play an important role in pedogenic processes, favoring larger spatial homogeneity compared with the concave curvature (Montanari et al., 2008). Conversely, the slightest value range in the concave hillslope curvature (Table 2) confirmed the greater variability by the highest CV values in this area (Table 1). The value ranges were 30.79 m and 41.0 m for Gt; 30.50 m and 50.0 m for Hm in concave and convex areas without data transformation, respectively (Table 2). Data processing for a standard normal distribution with zero mean and unit variance (eq. 7) did not change the spatial continuity of the Fe oxides contents. The value ranges were 30.00 m and 40.82 m for Gt, 28.76 m and 54.50 m for Hm in concave and convex hillslope curvature, respectively (Table 2). Therefore, the standardized variogram remained similar after changing the oxide of the experimental variogram. Delbari et al. (2009), assessed the uncertainty of water availability in soil,

and reported that the normal transformation of the observed data did not alter sample intrinsic spatial characteristic. According to Kim et al. (2008), relief is a major feature in determination of spatial distribution of soil attributes. Furthermore, using a numerical classification method and the digital elevation model for soil attribute distribution, Silva Júnior et al. (2012b) found that the spatial variability of soil attributes are dependent on landscape models. The SDDs of Fe oxides sample and standardized data (Table 2) were classified as moderate in both areas (Cambardella et al., 1994). The Hm and Gt contents had a high nugget effect in both areas, suggesting that there may be non-detected spatial variability within short sampling distance (10 m) combined with possible laboratory measurement, sampling errors and others.

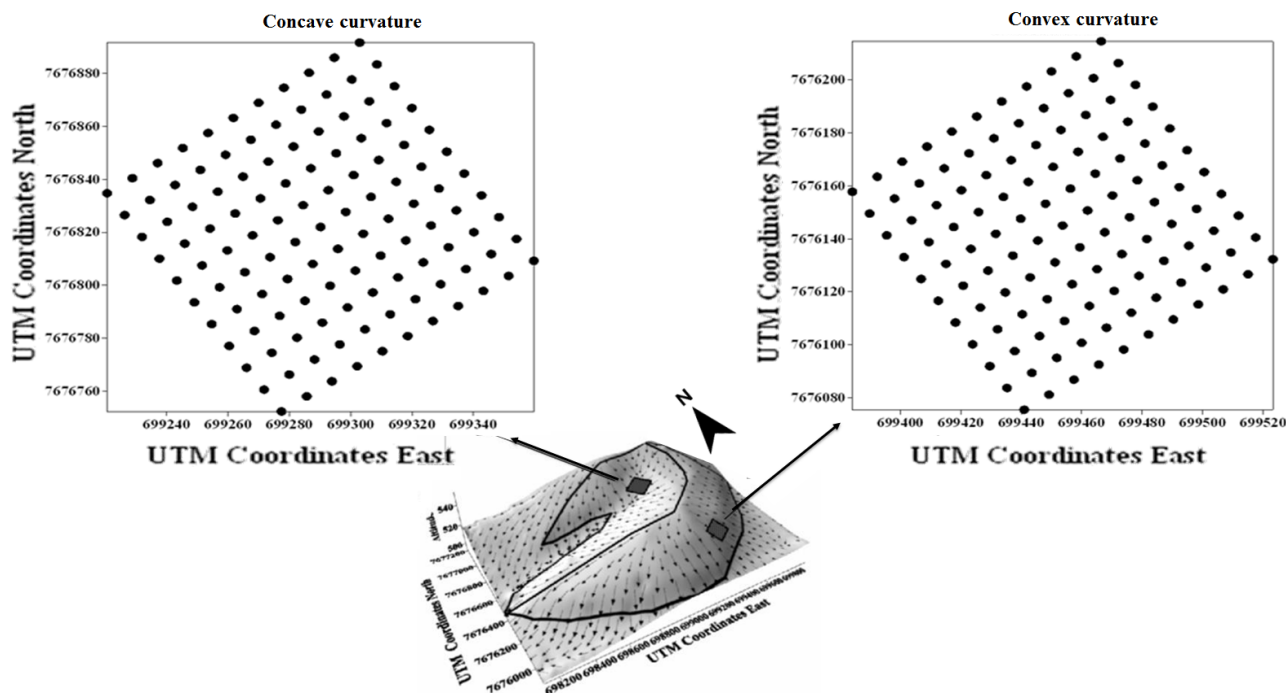
Interpolation maps and validation indexes

The marked squares in the delineation maps of each Fe oxide for both hillslope curvatures show overall visual differences of the two tested methods for spatial characterization (Fig 2). These maps show that OK under-estimates the Gt content in convex hillslope curvature, compared to TGK. Therefore, OK-estimated lower concentrations do not express real values. Also, such fact may interfere, when applied for a site-specific phosphate fertilizer application, in view of phosphorus and oxide under-estimation, so providing deficient amounts for each plant, since phosphorus amount is determined by Fe oxides. Lookman et al. (1995) points out negative results of under-estimation and over-estimation for sorption capacity of Fe and Al oxides using OK estimation. After estimating Hm and Gt content through OK and TGK, it was performed a validation of the maps (Table 3). The ME values were negative for the Gt and positive for Hm in both evaluated methods, indicating over-estimation (positive values) or under-estimation (negative values) to the spatial predictions (Chirico et al., 2007). The RMSE values were higher for the Hm and Gt in the concave curvature in both methods, except for OK estimates of Hm content. This may happen because of the greater variance of this oxide in the referred environment influencing a negative impact on the model ability. The RMSEr values were less than 40% for Gt content in the convex area estimated by both methods, and Hm content in both areas estimated by TGK and in concave estimated by OK. Thus, it indicates that the models explain more than 85% of the variability of the dataset validation (Hengl, 2009). The smallest RMSEr values were found for the oxides in the convex hillslope curvature, except for OK estimates of Hm that was 1.07. Relative improvement (RI) was positive for TGK estimates, showing improvement of 0.84 and 11.1% for the Gt and 8.23 and 0.76% for the Hm content in concave and convex hillslope curvature, respectively (Table 3). This might reinforce the hypothesis that TGK has greater advantages over OK in a more realistic representation of Fe oxide mapping. These results agree with McGrath et al. (2004) that found efficiency of box-cox transformation of data to weaken negative effect of outliers. For both methods, Fe oxide contents in the convex curvature presented mean G values of 0.6, which is near 1, indicating better accuracy of conditional cumulative distribution function (CCDF). Moreover, it was possible to observe that TGK G value is about 10% higher than the OK one (Table 3). This, again, reinforces Cressie and Hawkins (1980) hypothesis on a negative influence of higher variance values

Table 1. Descriptive statistics for the iron oxide contents in the studied soil samples.

Hillslope curvatures	Mean	Median	Min ^a	Max ^b	SD ^c	CV ^d	Skewness	Kurtosis	p ^e
	Goethite content (g kg ⁻¹)								
Concave	10.52	10.35	0.80	23.90	3.82	36.39	0.39	1.44	0.04
Convex	13.24	13.13	7.14	23.52	3.02	22.80	0.45	0.60	0.72
	Hematite content (g kg ⁻¹)								
Concave	12.47	12.70	0.70	28.60	4.29	34.40	0.63	3.50	<0.01
Convex	23.20	23.10	12.92	33.29	3.78	16.29	0.14	0.06	0.72

(N=108); ^aMinimum; ^bMaximum; ^cStandard deviation; ^dCoefficient of variation (%); ^ep >0.05 (normal distribution, Anderson–Darling test).

**Fig 1.** Digital elevation model, location of the studied area and the sampling grids in concave and convex hillslope curvatures.

to the variogram models; and consequently, the performance of spatial interpolators. Additionally, Zwervaegher et al. (2013) proved that an increased model quality will probably affect regression kriging. A TGK major efficiency was indicated by ϵ values to reproduce the experimental variogram of reference as long as they are near zero, especially in convex hillslope curvature, except for the Gt in concave hillslope curvature. It could be related to the high kurtosis value (1.44) for the Gt content in the concave hillslope curvature. Therefore, the theory of Webster and Oliver (2009) proved that variogram models are sensitive to outliers, so data transformation is recommended. Thus, it was proven that TGK is indicated for oxides with higher variability for a better decision making with respect to mapping efficiency by geostatistical methods. Characterizing spatial variability of Fe oxides in landscapes is essential since landscape models are designed to predict this mineral distribution in soil and spatial modeling. In addition, the knowledge on landscape important properties such as land surface, homogeneity and various discontinuity types at natural boundaries between geomorphic units are crucial (Minár and Evans et al., 2008). Therefore, spatial variability is landscape model dependent (Silva Júnior et al. 2012a, b). Such a fact importance was confirmed by Siqueira et al. (2010), who concluded that hillslope curvatures divisions helped to understand the relationship between physical and hydrologic soil attributes, influencing citrus yield. Later, Camargo et al. (2012) verified that slight hillslope curvature identification is valuable to understand their influence on soil

organic matter and available phosphorus contents, as well as kaolinite and Fe and Al oxide attributes. This reinforces that OK maps for Fe oxides should be used cautiously due to its uncertainty, especially in different slight hillslope curvatures. It can; therefore, be assumed that there is no "flawless" spatial interpolator since a "best" method works just at specific situations (Isaaks and Srivastava, 1989). However, the findings of the current study state that TGK maps are more preferable than OK, as long as the first brings higher accuracy, especially for convex hillslope curvature, or in any data with outlier values. Zhu and Lin (2010) compared the ordinary kriging and regression kriging for soil, and reported that Ok being generally preferable in the gently-rolling agricultural landscape. Thus, if the planner chooses the OK method for convex hillslope curvature maps, it may induce errors in decision-making processes related to soil management and Fe oxides.

Materials and Methods

The study area and soil sampling

The study area was located in Catanduva city, Northwestern São Paulo State, Brazil, at 21° 05' S latitude and 49° 01' W longitude. According to the Köppen method, the local climate is classified as hot humid tropical type (*Aw*); with dry winter; annual average rainfall of 1,350 mm; and temperature of 23 °C (above 22 °C in the warmest month and 18 °C in the coldest one); and relative humidity of 74%. The nature of soil

Table 2. Variogram parameters of spherical model to the standardized and experimental data of soil iron oxides.

Hillslope curvatures	C_0^a	$C_0+C_1^b$	a^c	$C_0/(C_0+C_1)^d$	R^2	RSS ^e
(sample) Goethite content						
Concave	3.90	12.60	30.79	30.95	0.82	1.38
Convex	3.28	13.10	41.00	25.03	0.90	5.21
(sample) Hematite content						
Concave	3.19	10.10	30.50	46.17	0.79	1.73
Convex	4.29	10.20	50.00	42.05	0.91	1.60
Standardized Goethite content						
Concave	0.23	0.68	30.00	28.39	0.92	2.8×10^{-3}
Convex	0.47	0.84	40.82	55.95	0.89	7.2×10^{-3}
Standardized Hematite content						
Concave	0.38	0.76	28.76	49.93	0.74	7.3×10^{-3}
Convex	0.37	0.77	54.50	47.73	0.94	5.9×10^{-3}

(N=108); ^aNugget effect; ^bSill; ^cRange (m); ^dDegree of spatial dependence; ^eResidual sum of square

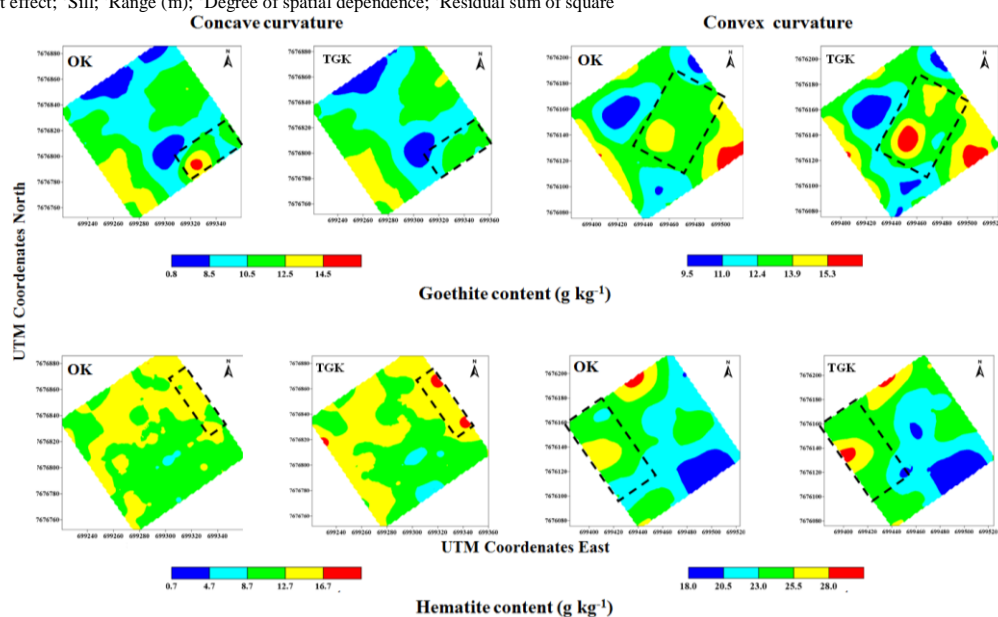


Fig 2. Spatial pattern of goethite and hematite contents (g kg^{-1}) in concave and convex hillslope curvatures by ordinary kriging (OK) and trans-Gaussian kriging (TGK).

Table 3. Mean error index (ME), root of mean squared error (RMSE), relative root of mean squared error (RMSEr), relative improvement (RI), reproduction of conditional cumulative distribution function (G) and accuracy in the reproduction of the variogram (ϵ) for iron oxides calculated from the external validation in concave and convex hillslope curvature.

Validation	Hillslope curvatures	TGK ^a	OK ^b	TGK	OK
		Goethite content		Hematite content	
ME	Concave	-0.63	-0.86	0.58	0.32
	Convex	-0.68	-0.65	0.63	10.78
RMSE	Concave	4.77	4.73	1.56	1.70
	Convex	0.40	0.45	1.17	4.05
RMSEr	Concave	1.25	1.24	0.36	0.40
	Convex	0.13	0.15	0.31	1.07
RI	Concave	0.84	-	8.23	-
	Convex	11.11	-	0.76	-
G	Concave	0.64	0.53	0.30	0.30
	Convex	0.69	0.57	0.60	0.54
ϵ	Concave	5.74	5.20	3.17	5.57
	Convex	4.37	5.14	2.95	4.25

(N=13); ^aTrans-Gaussian kriging; ^bOrdinary kriging.

source materials is defined as sedimentary sandstone rocks from the Bauru Group, Adamantina Formation (IPT, 1981). The soil was classified as Typic Hapludalf (Soil Survey Staff, 1999). Local natural (primary) vegetation is classified as a closed tropical rainforest, currently being cropped with sugarcane mainly, and under 20-year burn harvest. Area characterization was made through aerial photographs on a 1:35,000 scale, describing altimetric profile and performing geomorphological and pedological classification. Field measurements helped in hillslope curvature classification as described by Troeh (1965), using a designed digital elevation model (DEM) (Fig 1). Two areas were observed, one with convex and another with concave hillslope curvatures. So, in each area a 1^{ha} sample grid was defined with regular spacing of 10 x 10 m, totalizing 121 georeferenced sample points per area (Camargo et al., 2010).

Mineralogical analysis

The soil samples were treated with NaOH 0.5 N and subjected to mechanical stirring for 10 minutes to disperse particles. Following this pre-treatment, a 0.05 mm sieve was used to separate the sand fraction. Then, a centrifugation at 1,600 rpm divided the silt and sand fractions. The operation time was based on temperature at the analysis time. The clay suspension was flocculated with concentrated HCl and centrifuged at 2,000 rpm for 2 minutes. Next, the Fe oxides were extracted with sodium dithionite-citrate-bicarbonate (Fed) following the method proposed by Mehra and Jackson (1960). The Gt and Hm were determined through X-ray diffraction, held after clay treatment with 5-mol L⁻¹ NaOH (100 ml solution/ 1 g clay), according Norrish and Taylor (1961) and modified by Kämpf and Schwertmann (1982).

The Gt/ (Gt+Hm) ratio was calculated using the sample diffractogram of the area under the Hm (012) and Gt (110) reflexes. From this ratio, the Gt-110 reflection area was multiplied by 0.35 because the intensity of the Hm-012 is 35% (Kämpf and Schwertmann, 1998). The Fed% was converted into Gt content when multiplied by the Gt/(Gt + Hm) and then by 1.59. Subsequently, Hm content was found by subtracting the Fe% from FedGt% and multiplying by 1.43, as the equations below:

$$[Gt/(Gt + Hm)] \times Fed\% = FeGt\% \quad (\text{Eq. 1})$$

$$FeGt\% \times 1,59 = FeOOH = Gt\% \quad (\text{Eq. 2})$$

$$Fed\% - FeGt\% = FeHm\% \quad (\text{Eq. 3})$$

$$FeHm\% \times 1,43 = Fe_2O_3 = Hm\% \quad (\text{Eq. 4})$$

Statistical and geostatistical analysis

Initially, iron oxide variability was evaluated by descriptive statistics (mean, median, standard deviation, CV, skewness, kurtosis and normality test). The variability is classified as low for CV ≤ 12%, medium for 12% < CV ≤ 62% and high for CV > 62% (Warrick and Nielsen, 1980). Later, Gt and Hm spatial dependence were evaluated by experimental variograms, which were based on a stationarity intrinsic hypothesis (Deutsch and Journel, 1998) and could be estimated by:

$$\hat{\gamma}(h) = \frac{1}{2N(h)} \sum_{i=1}^{N(h)} [Z(x_i) - Z(x_i + h)]^2 \quad (\text{Eq. 5})$$

Where, $\hat{\gamma}(h)$ is the semivariance value at h distance; $N(h)$ is the number of point pairs $[Z(x_i), Z(x_i + h)]$ separated by an h distance; and x_i is the spatial position of the Z variable. The experimental variogram is represented by semivariance versus h graphic, from where a mathematical model can be

adjusted, through which coefficient of theoretical model were estimated: nugget effect (C_0), sill ($C_0 + C_I$) and ranger (a).

The data fit to a mathematical model is the most important step in a geostatistic study. In this study, models with the number of pairs equals or greater than 50 points to achieve higher degrees of representativeness in modeling procedure was adopted (Wollenhaupt et al., 1997; Burrough and McDonnell, 1998). Journel and Huijbregts (1978) recommended at least 30 pairs of points per interval for a proper semivariance estimation.

The ratio between nugget effect and sill $[C_0/(C_0 + C_I) \times 100]$, expressed as a percentage, is used to express spatial dependence degree (SDD), being classified as strong (≤ 25%), moderate (between 25 and 75%), and weak (> 75%) (Cambardella et al., 1994). The best-adjusted model is chosen based on residual sum of square (RSS), determination coefficient (R^2) and cross-validation parameters, which are obtained from a regression adjustment between the observed values and those predicted by modelling.

Ordinary kriging

Ordinary Kriging (OK) is used to estimate spatial variables without bias and under mild variance, non-sampled points by means of data interpolation (Webster and Oliver, 2009). A permissible theoretical model was adjusted, which was used for Gt and Hm estimations at non-sampled sites of the studied area. The OK estimation is given by the equation:

$$\hat{Z}(x_0) = \sum_{i=1}^n \lambda_i Z(x_i) \quad \text{with the constraint} \\ E\left\{ \left[\hat{Z}(x_0) - Z(x_0) \right] \right\} = 0 \quad \text{and} \quad \sum_{i=1}^n \lambda_i = 1 \quad (\text{Eq. 6})$$

Where in, $\hat{Z}(x_0)$ is an estimated OK from non-sampled points; X_0 , the observed value at i point, where $i=1,2,\dots,n$ and λ_i the weight associated to each nearest point in the value estimate, more details can be seen in Goovaerts (1997).

Trans-Gaussian Kriging

Trans-Gaussian Kriging (TGK) is an interpolation method of standardized score of non-observed random variables. The first step is to process the soil attribute data using the normal standard method, which is a graphical transformation that allows variables to have a normalized distribution independently of the initial one. The soil attributes were directly transformed to be standard normally distributed, subtracting the mean and dividing it by the standard deviation, that is:

$$Z_s(x_i) = \frac{Z(x_i) - \bar{Z}(x)}{\sigma(x)} \quad (\text{Eq. 7})$$

Wherein, $Z_s(x_i)$ is the attribute $Z(x)$ value at i point after standardization; $\bar{Z}(x)$ is $Z(x)$ value means; and $\sigma(x)$ is the standard deviation of $Z(x)$. Additionally, this standardization is called Z-score, in reference to a standard normal distribution. Such transformation was performed apart from kriging and variograms were calculated from the processed values, then, estimated by OK process, which is called TGK. After estimation via TGK, the values are again transformed back to the original scale (back-transformation).

Estimate validation

Thirteen observations, about 10% of all sampled points, were used for external validation (Teixeira et al., 2011) to evaluate

estimation accuracy of OK and TGK methods. In this procedure, the indexes mean error (ME) (Eq. 8), root of mean square error (RMSE) (Eq. 9) and the relative root of mean square error (RMSEr) were calculated (Eq. 10).

$$ME = \frac{1}{n} \sum_{i=1}^n [\hat{Z}(x_i) - Z(x_i)]; \text{ with } E\{ME\} = 0 \quad (\text{Eq. 8})$$

$$RMSE = \sqrt{\frac{1}{n} \sum_{i=1}^n [\hat{Z}(x_i) - Z(x_i)]^2};$$

$$\text{with } E(RMSE) = 0 \quad (\text{Eq. 9})$$

$$RMSEr(\%) = \frac{RMSE}{\sigma_z} \quad (\text{Eq. 10})$$

Where; n is the number of validation points ($n = 13$); $\hat{Z}(x_i)$ is the estimated value at i point; $Z(x_i)$ is the observed value at i point; and σ is the standard deviation of dataset ($n=108$). The smaller the RMSEr value, the more efficient modeling can be considered (Hengl, 2011).

The relative improvement (RI %) of TGK over the standard estimation method (OK) was calculated as follows:

$$RI = \frac{100 (RMSE_{OK} - RMSE_{TGK})}{RMSE_{OK}} \quad (\text{Eq. 11})$$

Where, $RMSE_{OK}$ and $RMSE_{TGK}$ are the root of mean square error values for the reference method (OK) and the TGK, respectively. If RI is positive, the evaluated method (TGK) accuracy will be greater than the reference one (OK) and vice versa (Zhang et al., 1992).

The G statistic was used to quantify how well conditional cumulative distribution function (CCDF) of a geostatistics method plays in the CCDF sample data (Herbst et al. 2009). Knowing the CCDF of each interpolated set allows computing symmetric probability intervals (IP-p) limited by $(1-p)/2$ and $(p+1)/2$ for any accumulated probability at a u site. The true value fractions within an IP-p-symmetrical can be calculated, knowing the interpolated data CCDF $\hat{F}(u, z/(n)), j = 1, \dots, N$ and sample data

$$Z(u_j), j = 1, \dots, N : \bar{\xi}(p) = \frac{1}{N} \sum_{j=1}^N \xi(u_j, p) \forall p \in [0,1]; \quad (\text{Eq. 12})$$

Where,

$$\xi(u_j, p) = \begin{cases} 1 & \text{if } F^{-1}(u_j, (1-p)/2) < z(u_j) \leq F^{-1}(u_j, (1+p)/2) \\ 0 & \text{otherwise} \end{cases}$$

The correlation between estimated fraction and sampled fraction was obtained by G statistics.

$$G = 1 - \int_0^1 [3a(p) - 2][\bar{\xi}(p) - p] dp \quad (\text{Eq. 13})$$

$$\text{Where, } a(p) = \begin{cases} 1 & \text{if } \bar{\xi}(p) \geq p \\ 0 & \text{otherwise} \end{cases}$$

In non-accurate cases ($\bar{\xi}(p) < p$), $a(p)$ values promote weighting twice that accurate cases, when $\bar{\xi}(p) \geq p$. The best CCDF is represented by a G values near 1.

The variogram reproduction accuracy was evaluated by ε_y statistics (Goovaerts, 2000).

$$\varepsilon_y = \sum_{s=1}^S \frac{[y(h_s) - \hat{y}(h_s)]^2}{[y(h_s)]^2} \quad (\text{Eq. 14})$$

Where, S is the number of lags used to build the variogram;

$\hat{y}(h_s)$ is the semivariance at h_s distance calculated from the estimated values by the interpolation method; $y(h_s)$ is the semivariance value of the fitted model at h_s distance. Due to square division, more emphasis is given to following source model, which is shorter h distances, as the interpolation calculations are more relevant for this region. Values close to zero indicate good accuracy in the reproduction of the variogram (Bourennane et al., 2007).

Conclusion

Trans-Gaussian Kriging has better performance for estimations when compared to Ordinary Kriging; therefore, it is recommended for iron oxide mapping in both convex and concave hillslope curvatures. Hillslope curvature classification has great importance as variogram modeling concerning method efficiency. It may improve the geostatistical mapping of iron oxides. Ordinary Kriging maps for iron oxides should be cautiously used due to its uncertainty, especially in other hillslope curvature. The Ordinary Kriging being generally preferable in the gently-rolling agricultural landscape

Acknowledgements

Financial support provided by Coordination for the Improvement of Higher Education Personnel (CAPES) is gratefully acknowledged.

References

- Bigham JM, Fitzpatrick RW, Schulze D (2002) Iron oxides. In: Dixon JB, Schulze DG (eds) Soil mineralogy with environmental applications, 2nd edn. Soil Science Society of America Book Series, Madison.
- Bourennane H, King D, Couturier A, Nicoulaud B, Mary B, Richard G (2007) Uncertain assessment of soil water content spatial patterns using geostatistical simulations: An empirical comparison of a simulation accounting for secondary information. *Ecol Model.* 205:323-335.
- Burrough PA, McDonnell RA (1998) Principles of geographical systems. Oxford University Press, New York. p 333.
- Camargo LA, Marques JR J, Pereira GT, Alleoni LRF (2012) Spatial correlation between the composition of the clay fraction and contents of available phosphorus of an Oxisol at hillslope scale. *Catena.* 100:100-106.
- Camargo LA, Marques JR J, Pereira GT (2013a) Mineralogy of the clay fraction of Alfisols in two slope curvatures. III - Spatial variability. *Rev Bras Cienc Solo.* 37:295-306.
- Camargo LA, Marques JR J, Pereira, GT (2013b) Mineralogy of the clay fraction of Alfisols in two slope curvatures. IV - Spatial correlation with physical properties. *Rev Bras Cienc Solo.* 37:307-316.
- Camargo LA, Marques JR J, Pereira GT, Horvat RA (2008) Variabilidade espacial de atributos mineralógicos de um Latossolo sob diferentes formas de relevo. I-Mineralogia da fração argila. *Rev Bras Cienc Solo.* 32:2269-2277.
- Camargo LA, Marques JR J, Pereira GT (2010) Spatial variability of attributes of an alfisol under different hillslope curvatures. *Rev Bras Cienc Solo.* 34:617-630.
- Cambardella CA, Moorman TB, Novak JM, Parkin TB, Karlen DL, Turco RF, Konopka AE (1994) Field-scale variability of soil properties in central Iowa soils. *Soil Sci Soc Am J.* 58:1501-1511.

- Campos MCC, Cardozo NP, Marques JR J (2006) Modelos de Paisagem e sua Utilização em Levantamentos Pedológicos. *Rev Biol Ciênc Terra*. 6:104-114.
- Chirico GB, Medina H, Romano N (2007) Uncertainty in predicting soil hydraulic properties at the hillslope scale with indirect methods. *J Hydrol*. 334:405-422.
- Cressie N, Hawkins DM (1980) Robust estimation of the variogram: I. *Math Geol*. 12:115-125.
- Cressie, N (1993) *Statistics for Spatial Data*. Revised Ed. John Wiley and Sons, New York.
- Cunha P, Marques JRJ, Curi N, Pereira GT, Lepsch IF (2005) Superfícies geomórficas e atributos de latossolos em uma seqüência arenítico-basáltica da região de Jaboticabal (SP). *Rev Bras Cienc Solo*. 29:81-90.
- Delbari M, Afrasiab P, Loiskandl W (2009) Using sequential Gaussian simulation to assess the field-scale spatial uncertainty of soil water content. *Catena*. 79:163-169.
- Deutsch CV, Journel AG (1998) *GSLIB: Geostatistical Software Library: And User's Guide*, 2th Ed. Oxford University Press, New York. p 369.
- Emery X (2006) Ordinary multigaussian kriging for mapping conditional probabilities of soil properties. *Geoderma*. 132:75-88.
- Goovaerts P (2001) Geostatistical modeling of uncertainty in soil science. *Geoderma*. 103:3-26.
- Goovaerts P (2000) Estimation or simulation of soil properties? An optimization problem with conflicting criteria. *Geoderma*. 97:165-186.
- Goovaerts P (1997) *Geostatistics for Natural Resources Evaluation*. Oxford University Press, New York. p 483.
- Goovaerts P (1999) *Geostatistics in soil science: state-of-the-art and perspectives*. *Geoderma*. 89:1-45.
- Hengl T (2011) *A Practical Guide to Geostatistical Mapping*, 2th Ed. University of Amsterdam. p 291.
- Herbst M, Prolingheuer N, Graf A, Huisman JA, Weihermüller L, Vanderborcht J (2009) Characterization and understanding of bare soil respiration spatial variability at plot scale. *Vadose Zone J*. 8:762-771.
- Inda Júnior AV, Kämpf N (2005) Variabilidade de goethita e hematita via dissolução redutiva em solos de região tropical e subtropical. *Rev Bras Cienc Solo*. 29:851-866.
- Instituto de Pesquisas Tecnológicas do Estado de São Paulo (1981) *Mapa Geológico do Estado de São Paulo*. Escala - 1:500.000. São Paulo, ITP.
- Isaaks EH, Srivastava RM (1989) *An Introduction to Applied Geostatistics*. Oxford University Press, New York, p 561.
- Journel A G, Huijbregts CJ (1978) *Mining geostatistics*. London: Academic press, 600 p.
- Kämpf N, Curi N (2000) Óxidos de ferro: Indicadores de atributos e ambientes pedogênicos e geoquímicos. In: Novais RF, Alvarez V, Schaefer CEGR (eds) *Tópicos em ciência do solo*, 2nd edn. Sociedade Brasileira de Ciência do Solo, Viçosa.
- Kämpf N, Schwertmann U (1982) Goethite and hematite in a climosequência in Southern Brazil and their application in classification of kaolinitic Soils. *Geoderma*. 29:27-39.
- Kämpf N, Schwertmann U (1998) Avaliação da estimativa de substituição de Fe por Al em hematitas de solos. *Rev Bras Cienc Solo*. 22:209-213.
- Kerry R, Oliver MA (2007) Determining the effect of asymmetric data on the variogram. I. Underlying asymmetry. *Comput Geosci*. 33:1212-1232.
- Kim D, Yu BK, Park SJ (2008) Identification and visualization of complex spatial pattern of coastal dune soil properties using gis-based terrain analysis and geostatistics. *J Coastal Res*. 24:50-60.
- Lookman R, Vandeweert N, Merckx R, Vlasak K (1995) Geostatistical assessment of the regional distribution of phosphate sorption capacity parameters (Feox and Alox) in northern Belgium. *Geoderma*. 66:285-296.
- McBratney AB, Webster R (1986) Choosing functions for semi-variograms of soil properties and fitting them to sampling estimates. *Eur J Soil Sci*. 37: 617-639.
- McGrath D, Zhang C, Carton OT (2004) Geostatistical analyses and hazard assessment on soil lead in Silvermines área. *Ireland. Environ Pollut*. 127:239-248.
- Minár J, Evans IS (2008) Elementary forms for land surface segmentation: The theoretical basis of terrain analysis and geomorphological mapping. *Geomorphology*. 95:236-259.
- Montanari R, Pereira GT, Marques JR J, Souza ZM, Pazeto RJ, Camargo LA (2008) Variabilidade espacial de atributos químicos em Latossolo e Argissolos. *Cienc Rural*. 38:1266-1272.
- Montanari R, Marques JR J, Campos MCC, Souza ZM, Camargo LA (2010) Caracterização mineralógica de Latossolos em diferentes feições do relevo na região de Jaboticabal, SP. *Rev Ciênc Agron*. 41:191-199.
- Mehra OP, Jackson ML (1960) Iron oxide removal from soils and clay by a dithionite-citrate system bulfered with sodium bicarbonate. *Clay Clay Miner*. 7:317-327.
- Norrish K, Taylor RM (1961) The isomorphous replacement of iron by aluminum in soil goethites. *J Soil sci*. 12:294-306.
- Robinson TP, Metternicht G (2006) Testing the performance of spatial interpolation techniques for mapping soil properties. *Comput Electron Agr*. 2:97-108.
- Schwertmann U, Taylor RM (1989) Iron oxides. In: Dixon JB, Weed SB (eds) *Minerals in soil environments*, 2nd edn. Soil Science Society of America Book Series, Madison.
- Silva Júnior JF, Marques JR J, Camargo LA, Teixeira DDB, Panosso AR, Pereira GT (2012a) Simulação geoestatística na caracterização espacial de óxidos de ferro em diferentes pedoformas. *Rev Bras Cienc Solo*. 36: 1690-1703.
- Silva Júnior JF, Siqueira DS, Marques JR J, Pereira GT (2012b) Classificação numérica e modelo digital de elevação na caracterização espacial de atributos dos solos. *Rev Bras Eng Agr Amb*. 16:415-424.
- Siqueira DS, Marques Júnior J, Pereira GT 2010 The use of landforms to predict the variability of soil and orange attributes. *Geoderma*. 155:55-66.
- Soil Survey Staff (1999) *Soil Taxonomy: A basic system of soil classification for making and interpreting soil surveys*. 2th.ed. Washington. p 869.
- Teixeira DDB, Panosso AR, Cerri CEP, Pereira GT, La Scala N (2011) Soil CO₂ emission estimated by different interpolation techniques. *Plant Soil*. 345:187-194.
- Troeh FR (1965) Landform equations fitted to contour maps. *Amer J Sci*. 263: 616 - 627.
- Warrick AW, Nielsen DR (1980) Spatial variability of physical properties in the field. In: Hillel D (ed), *Applications of Soil Physics*, Academic Press, New York, 1980.
- Webster R, Oliver M (2009) *Geostatistics for Environmental Scientists Statistics in Practice*. Wiley, 2th Ed. Chichester, p 315.
- Wollenhaupt NC, Mulla DJ, Crawford G (1997) Soil sampling and interpolation techniques for mapping spatial variability of soil properties. In: Pierce FJ, Sadler EJ (eds). *The state of site-specific management for agriculture*. Madison: ASA, CSSA, SSSA, p.19-53.
- Wilding LP, Drees LR (1983) Spatial variability and pedology. In: Wilding LP, Smeck NE, Hall GF (Eds) *Pedogenesis and soil taxonomy I: concepts and*

- interactions. Elsevier Science Publishing Company, New York, pp 83-116.
- Yamamoto JK, Chao L (2009) Comparação de métodos para teste de bigaussianidade. *Geociências*. 28:121-128.
- Zhang R, Warrick AW, Myers DE (1992) Improvement of the prediction of soil particle size fractions using spectral properties. *Geoderma*. 52:223-234.
- Zhu Q, Lin HS (2010) Comparing ordinary kriging and regression kriging for soil properties in contrasting landscapes. *Pedosphere* 20: 594–606.
- Zwertvaeghera A, Finke P, Smedt PD, Gelorinia V, Van Meirvenne M, Batsc M, Reuc JD, Antropd M, Bourgeois J, Maeyerd PD, Verniersa J, Crombéc P (2013) Spatio-temporal modeling of soil characteristics for soilscape reconstruction. *Geoderma*. 207-208:166–179.